

Colloid-polymer mixtures in the protein limit

Peter G. Bolhuis, Evert Jan Meijer and Arnd A. Louis²

Dept. of Chemical Engineering, University of Amsterdam,
Nieuwe Achtergracht 166, 1018 WV, Amsterdam, Netherlands

²Dept. of Chemistry, University of Cambridge, Lensfield Road, CB2 1EW, Cambridge, UK
(Dated: March 22, 2024)

We computed the phase-separation behavior and effective interactions of colloid-polymer mixtures in the "protein limit", where the polymer radius of gyration is much larger than the colloid radius. For ideal polymers, the critical colloidal packing fraction tends to zero, whereas for interacting polymers in a good solvent the behavior is governed by a universal binodal, implying a constant critical colloid packing fraction. In both systems the depletion interaction is not well described by effective pair potentials but requires the incorporation of many-body contributions.

PACS numbers: 82.35.Np, 61.25.Hg, 82.70.Dd

Adding polymers to suspensions of micro- and nanoparticles induces depletion interactions that profoundly affect their physical properties. This phenomenon has important scientific and (bio-)technological applications. Polymers such as polyethylene glycol are routinely added to protein solutions to enable protein crystallization [1, 2], a poorly understood process and of great importance in structural biology [3]. In cell biology depletion interactions are key in the process of macromolecular crowding [4]. Food and paint production are among the industrial sectors where depletion phenomena play a role.

In this Letter we focus on mixtures of hard sphere (HS) colloids with a radius R_c and non-adsorbing polymers with a radius of gyration R_g , in the regime where $q = R_g/R_c > 1$. This is often called the nano-particle or "protein limit", because in practice small particles such as proteins or micelles are needed to achieve large size-ratios q . Whereas the opposite "colloid limit" ($q < 1$) has been well studied, the physics in the protein limit is less established. This imbalance is partially due to the lack of well characterized experimental model systems for the protein limit and partially to a poor theoretical understanding. The colloid limit can be well described within the framework of effective depletion pair potentials [5, 6], in contrast to the protein limit, where the interactions cannot be reduced to a pairwise form [7, 8]. Nevertheless, for biological and industrial applications, this regime is at least as important as the colloid limit.

One of the first theoretical treatments of colloid-polymer mixtures in the protein limit was by de Gennes [9], who showed that the insertion free-energy $F_c^{(1)}$ of a single hard, non-adsorbing sphere into an athermal polymer solution scales as

$$F_c^{(1)} \propto (R_c)^{3-1/\nu} \quad (1)$$

when $R_c < R_g$, with the polymer correlation length $\xi_p = R_g/p^{1/\nu}$ [10]. Here, $\nu = 1/k_B T$ is the reciprocal temperature, 0.59 is the Flory exponent and $p = \phi_p^3 R_g^3$ is the polymer volume fraction for a polymer number density ϕ_p , so that

ϕ_p at the crossover from a dilute to a semi-dilute solution [10]. The prefactors can be calculated by the renormalization group (RG) theory [11], yielding: $F_c^{(1)} \approx 4.39 \phi_p^{1/3}$ which has been verified by computer simulations for small q [12]. Based on this description of $F_c^{(1)}$, de Gennes [10] and Odijk [8] predicted extensive miscibility for colloid-polymer mixtures in the large q limit if $R_c < R_g$. However, it is well known that protein-polymer mixtures do phase-separate [13, 14]. Recently, Odijk et al. [15] suggested that a poor solvent could facilitate phase-separation. Sear [16] altered the form of $F_c^{(1)}$ to include effects when $R_c > R_g$, and also predicted phase-separation with a truncated virial theory. The same author recently proposed an alternative theory [17] where the colloids induce depletion attractions between the polymers, leading to a poorer effective solvent and eventually phase-separation. Mean-field cell model calculations also predict demixing [18]. Another promising approach uses integral equation techniques [19] to predict spinodal curves and critical points. However, all these theories suffer from several uncontrolled approximations leading to different predictions for the causes and properties of the phase-separation. To clarify this situation, we performed computer simulations with as few simplifying assumptions as possible, on which we report in this Letter.

We have recently used a coarse-graining technique [20] to study the colloid limit, and found quantitative agreement with experimental fluid-fluid binodals [21], and significant qualitative differences between interacting (IP) and non-interacting (NIP) polymers. Here, we study the same athermal model of HS colloids and non-adsorbing polymers in the protein limit, and calculate, for the first time, the full fluid-fluid binodals by direct simulation. The results for the IP and NIP show even larger qualitative differences, and many-body depletion interactions must be invoked to understand the phase-behavior.

The simulation model consists of polymers on a simple cubic lattice mixed with HS colloids. The interacting polymers in a good solvent are modeled as self-avoid-

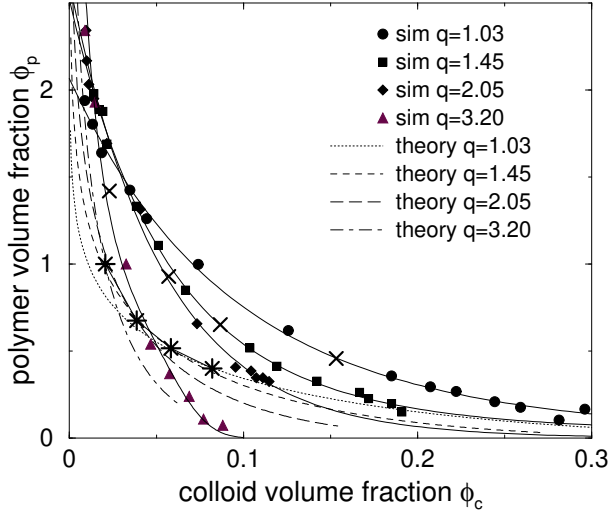


FIG. 1: Fluid-fluid binodals for a mixture of non-interacting polymers and HS colloids with different size-ratios q . Crosses indicate the estimated critical point, obtained by extrapolating the calculated phase boundaries. The full lines are a guide to the eye. Dashed lines denote the simple theory described in the text, with stars marking the critical points.

ing walks (SAW) of length L , which have a radius of gyration $R_g \sim L$. The non-interacting polymers are modeled as random-walks, for which $R_g \sim L^{0.5}$. In both models there is an excluded-volume interaction between the colloidal HS and the polymer segments. The simulations were performed on a D^3 lattice with periodic boundary conditions, where $D = 48$ and $D = 100$ for the NIP and IP system, respectively. Throughout this Letter, we use the lattice spacing as the unit of length. For the NIP the colloidal HS diameter was $\sigma_c = 5.5$ and the polymer length was $L = 50; 100; 200$ and 500 , corresponding to $q = 1.03; 1.45; 2.05$ and 3.2 , respectively. For the IP $L = 2000$, and $\sigma_c = 10; 14$ and 20 , yielding $q = 3.86; 5.58$ and 7.78 , respectively. Colloidal positions have continuous values, but when we calculated the interaction between colloid and polymer the colloids were shifted such that they occupied a constant number of lattice sites to prevent spurious attractive positions for single colloids (other lattice effects, although unavoidable, are expected to be small). Thermodynamic state points were calculated in the grand-canonical ensemble, i.e. at fixed volume V , colloid chemical potential μ_c and polymer chemical potential μ_p using Monte Carlo (MC) techniques. The NIP were sampled using an (exact) lattice propagation method [22, 23], while the IP configurations were generated using translation, pivot moves and configurational bias MC [24] in an expanded ensemble to facilitate insertion of long chains [25]. Typical simulations lengths are 10^9 Monte Carlo moves per state point. In order to determine the liquid-liquid binodals we first estimated the coexistence line by scanning a series of ϕ_c

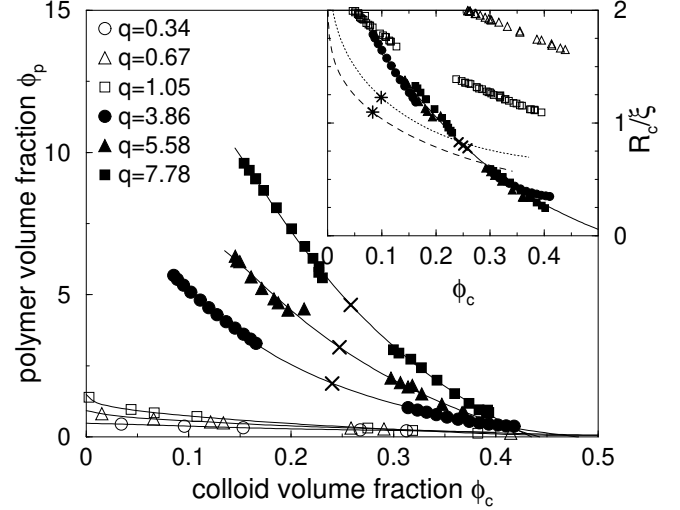


FIG. 2: Fluid-fluid binodals for a mixture of interacting polymers and HS colloids at different size-ratios q . Filled symbols are direct simulation data. The open symbols are the colloid limit ($q < 1$) results from Ref. [21]. Solid lines are a guide to the eye. Inset: The same binodals plotted in a reduced polymer density representation. The dotted curve corresponds to a simple theory for the universal binodal when polymers are in a good solvent while the dashed line is for polymers in a poorer solvent. Crosses and stars as in Fig. 1.

for several values of μ_p and locate the ϕ_c for which a sudden density change occurred. Subsequently 8-10 (μ_p, ϕ_c) coexistence state points were simulated simultaneously using parallel tempering [25]. When the estimated coexistence points are sufficiently close to the true binodal and to each other, and near the critical point, this scheme results in proper ergodic sampling of both phases. If necessary, the chemical potentials were adjusted towards coexistence. We used the multiple histogram reweighting [25, 26] technique to determine the precise location of the $(\phi_c; \mu_p)$ coexistence line, and the phase boundaries in the $(\phi_c; \mu_p)$ plane, where $\phi_c = \phi_c^4 / 3 R_c^3$ is the colloid volume fraction, with ϕ_c the colloid number density.

Figs. 1 and 2 contrast the calculated phase diagrams for NIP and IP for several size-ratios q . Firstly, we note that both models show extensive immiscibility, in agreement with experiment [14]. Secondly, the two systems exhibit striking differences: for the NIP, the critical colloid volume fraction ϕ_c^{crit} tends to zero with increasing size-ratio q , while the IP exhibit a nearly constant value of ϕ_c^{crit} . For both systems the critical polymer concentration ϕ_p^{crit} increases with increasing q . The phase separation occurs well into the semi-dilute regime for the IP, again in qualitative agreement with experiment [13]. Properties of semi-dilute polymer solutions are independent of polymer length, being instead determined by the correlation length ξ , which is a function of the monomer density $c = L \phi_p$. The phase behavior of the polymer-HS mixture

should therefore only be a function of the ratio $R_c = \phi_p / \phi_c$ [16]. Indeed, when the phase lines in Fig. 2 are rescaled with an accurate prescription for ϕ_p [12], the binodals nearly collapse onto a "universal binodal", as shown in the inset of Fig. 2. This explains why the critical colloid packing fraction is nearly constant in the simulations. Similarly, ϕ_p^{crit} scales as $\phi_p^{\text{crit}} \propto q^{3/2} \phi_c^{1/2}$. For comparison, we have also included results for $q < 1$ from Ref. [21] in Fig. 2. These results do not exhibit the same scaling behavior, since they are not in the semi-dilute regime.

The differences between NIP and IP phase behavior can be rationalized with some simple theories. Consider a Helmholtz free-energy F of the form $F = V = f = f_c^{\text{HS}} + f_p + f_{\text{cp}}$. Here, the HS free energy f_c^{HS} is given by the accurate Camahan-Starling expression [27], and the polymer free energy f_p for either IP or NIP solutions is well understood [10]. The contribution due to the HS-polymer interactions f_{cp} is non-trivial. A first approximation truncates after the second cross-virial coefficient, yielding $f_{\text{cp}} \approx \phi_c F_c^{(1)}$. For NIP the insertion free-energy $F_c^{(1)}$ is exactly known [11], so that f_{cp} takes the form $f_{\text{cp}}^{\text{id}} = \phi_p \phi_c [1 + \frac{6q}{3} + 3q^2] \phi_p \phi_c \hat{b}_{\text{cp}}$, which defines the reduced cross-virial coefficient \hat{b}_{cp} . Since $f_{\text{cp}}^{\text{id}}$ grows with increasing q , immiscibility sets in at lower colloid packing fraction ϕ_c . The theory can be improved by realizing that the polymers only exist in the free volume left by the colloids [28]. Simply taking this free volume to be $1 - \phi_c$ is an adequate first approximation for the protein limit. The trends for the binodal lines calculated from this simple theory, shown in Fig. 1, agree qualitatively with the simulations. For example, the critical point shifts to smaller ϕ_c and larger ϕ_p for increasing q , and the binodal lines cross at a low ϕ_c . For computational reasons the simulations only go up to $q = 3.2$ and we expect better quantitative agreement for larger q since ϕ_c^{crit} decreases so that the second-virial theory should become more accurate. In the $q \rightarrow 1$ limit, this theory yields $\phi_c^{\text{crit}} \rightarrow 1 - \hat{b}_{\text{cp}} = 1 - (3q^2)$, and $\phi_p^{\text{crit}} = q^3 \phi_c^{\text{crit}} = q^3$. Note that in the same limit, the penetrable sphere or Asakura-Oosawa model [28] scales somewhat differently: $\phi_c^{\text{crit}} \rightarrow 1 - q^3$ and $\phi_p^{\text{crit}} \rightarrow 1$. Sear [7] already pointed out the $\phi_c^{\text{crit}} \rightarrow 0$ behavior using a slightly different prescription for the free volume than we employ here. Here we claim that the limiting results are a general feature of free-volume theories.

In the IP case, f_{cp} is more difficult to estimate, even for a second cross-virial theory. The $R_c \rightarrow \infty$ limit is given by Eq. (1) with the prefactors from RG theory. For $R_c \rightarrow \infty$ we have previously shown that $F_c^{(1)}$ is given by $F_c^{(1)} = \frac{4}{3} R_c^3 + 6 R_c^2 \phi_s$ [12], where the polymer osmotic pressure ϕ_s is well known [10]. However, since Eq. (1) is essentially a surface (depletion layer) contribution, we use a simple approximate second cross-virial term $f_{\text{cp}} = \phi_c (\frac{4}{3} R_c^3 + 4.39 \phi_p q^{1/3})$, which

reduces to the correct form in both the $R_c \rightarrow \infty$ and the $R_c \rightarrow 0$ limit [33]. As with our treatment of NIP, we take the effect of the colloid excluded volume into account by computing the polymer densities in the free volume fraction $1 - \phi_c$ (see Ref. [29] for a complementary approach). The theoretical binodals were calculated using accurate expressions for ϕ_c and ϕ_p [12] and are compared with the simulation results in Fig. 2, in the $R_c = \phi_p / \phi_c$ versus ϕ_c plane. The qualitative agreement suggests that we can also use this theory to estimate the effect of a poorer solvent on the binodals. Following Ref. [15], we alter the scaling of ϕ_p to $\phi_p = \phi_c^3$ so that $\phi_p \propto \phi_c^3$. Interestingly, Fig. 2 shows that using $\phi_p = \phi_c^3$ instead of the appropriate exponent for polymers in a good solvent ($\phi_p \propto \phi_c^{2/3}$), does not result in important differences in the binodals. Of course, the differences will appear larger in the $(\phi_c; \phi_p)$ plane due to the different scaling of ϕ_p . One must keep in mind, however, that these predictions follow from a simple scaling theory and qualitatively different behavior may emerge when one approaches the $\phi_c = 1$ point (where $\phi_p = 1$).

To illustrate the many-body nature of the depletion interaction we estimated the phase behavior by approximating the system by colloids interacting via pairwise effective potentials. We computed the effective pair interaction $v(r)$ between two colloids in a bath of IP's, by $v(r) = -k_B T \ln g(r)$ for $\phi_c \neq 0$. The colloid radial distribution function $g(r)$ was estimated by measuring the insertion probability of a HS at a distance r from a second fixed HS in a SAW polymer solution using the above MC techniques. Results for a single size-ratio $q = 7.78$ as a function of ϕ_p are shown in Fig. 3. Several features are

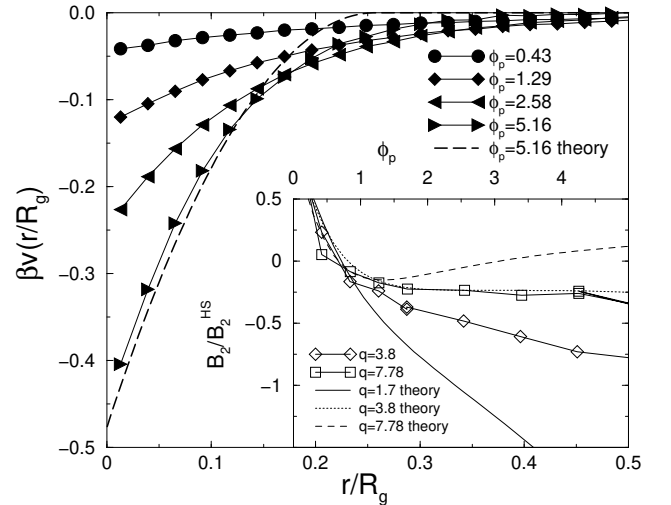


FIG. 3: Effective colloid-colloid pair potentials induced by interacting polymers for $q = 7.78$. Theoretical lines from Ref. [30]. Inset: Reduced second osmotic virial coefficient $B_2 = B_2^{\text{HS}} (\frac{2}{3} R_c^3)$ as a function polymer densities for several size ratio's.

